JRC Scientific and Technical Reports

Field evaluation of NanoEnvi microsensors for O_3 monitoring

M. Gerboles, I. Fumagalli, F. Lagler and S. Yatkin

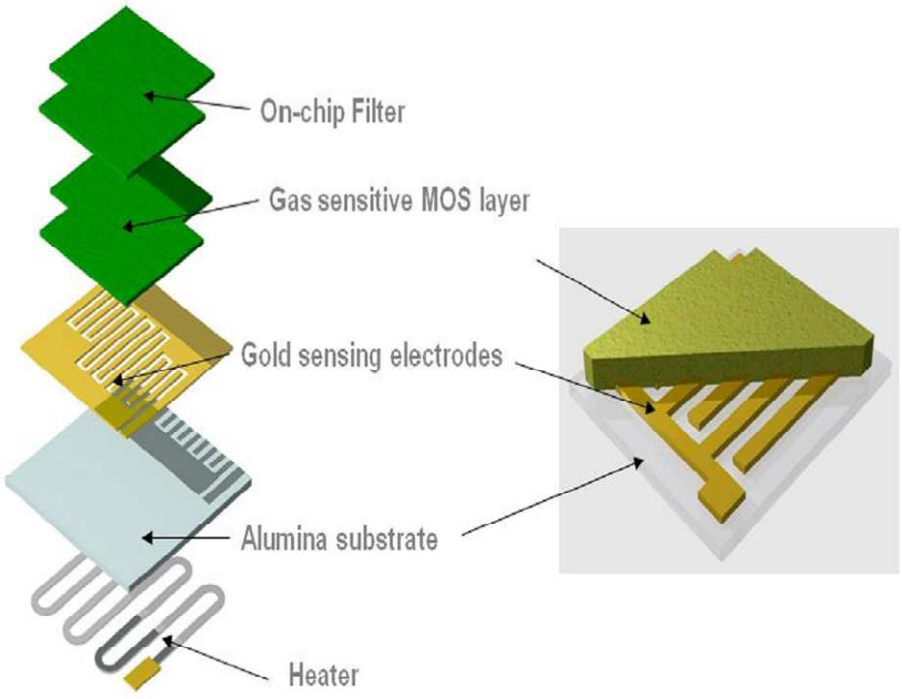

EUR 25156 EN - 2011

JRC
EUROPEAN COMMISSION

ies
Institute for Environment and Sustainability

The mission of the JRC-IES is to provide scientific-technical support to the European Union's policies for the protection and sustainable development of the European and global environment.

European Commission
Joint Research Centre
Institute for Environment and Sustainability

Contact information
Address: M. Gerboles, Joint Research Centre, TP 442, Via E. Fermi 2749, I -21027 Ispra
E-mail: Michel.gerboles@jrc.ec.europa.eu
Tel.: +39 0332 785652
Fax: +39 0332 789931

http://ies.jrc.ec.europa.eu/
http://www.jrc.ec.europa.eu/

JRC 68169

EUR 25156 EN
ISBN 978-92-79-22682-3
ISSN 1831-9424
doi:10.2788/44968

Luxembourg: Publications Office of the European Union, 2012

Printed in Italy

Summary

Previous studies have showed that microsensors can successfully measure ozone in ambient air for a limited period of time after on-site calibration by comparison to ultraviolet photometry. This method is generally more successful than experiments in exposure chambers under controlled conditions because of the difference between laboratory and fields air matrixes.

To expand this result, we carried out an experiment at two sampling sites. At the first site, the microsensors were calibrated during a few days. Subsequently, the calibrated microsensors were taken to another sampling site where the effectiveness of the calibration function of the first site was evaluated.

In this study, the calibration functions determined at the first site, in Ispra, could not be directly applied to the microsensor measurements at the second site, in Angera. The main finding of the campaign is the detection of a bias between the calibration in Ispra and the measurements in Angera. At low ozone concentrations, this bias was about 15-20 nmol/mol. However, we cannot be 100-percent sure that the malfunctioning is caused by microsensors since errors of the UV photometry method at any of the two sampling sites cannot be excluded. The bias could not be simply eliminated by a re-zero calibration because its magnitude depended on the ozone concentration levels.

By calibrating using measurements over the first 6 days of the measurement campaign in Angera, the microsensors were rather successful with daily bias in the range of 1 ± 2.3 nmol/mol (1s) and hourly bias in the range of 0.5 ± 4 nmol/mol (1s). However, for one microsensor, a sudden and abrupt change in its response took place at the end of the measuring campaign and it was not possible to find a reason for this change.

The magnitude of the bias and its relationship with ozone levels were different in the O_3-filtered OTC and in the un-filtered OTC suggesting a different matrix effect on the microsensor response.

Generally, calibration (sensor resistances versus ozone concentrations) using a simple linear model was sufficient once the sensor resistance was corrected for temperature effect. In some instance a 2^{nd} order models was necessary. At the first sampling site, the calibration function could be optimized by introducing a correction of the 1^{st} derivative of the resistance of the sensor. However, this sophisticated approach did not produce any improvement for the experiments in Angera.

Table of Contents

Acknowledgement:

The authors wish to thank Dr. Niels Roland Jensen and Alessandro Dell'Acqua of the ABC-IS/EMEP air quality monitoring station, Institute for the Environment and Sustainability, Climate Change and Air Quality Unit in Ispra (I) for making the air pollution data of the ABC-IS station available.

The authors are also grateful to Dr. Alejandro Junquera Perez of Ingenieros Asesores S.A., Llanera (Asturias - Spain) for making available the NanoEnvi microsensors, their solar cells and the data acquisition system that were tested in this study.

1 Introduction

A microsensor is a device that converts any non-electrical physical or chemical quantity, such as gas concentration, into an electrical signal. Microsensors are very small with physical dimensions in the sub-micrometer to millimeter range. They are generally based on the variation of conductance of a semi-conductor that changes with the concentration of a pollutant that is adsorbed on the semi conductor sensitive layer. Microsensors have been operated for monitoring ambient air pollution and in particular ozone (O_3) at concentrations of several 10s of nmol/mol since the end of the 80s[1,2,3,4,5]. They can be used for several purposes including checking limit values of Air Quality European Directives, near-to-real-time mapping of air pollution, rural or forest monitoring where power supply is not available (for example using accumulators or solar cells), validation of models of air pollution dispersion, evaluation of the exposure of population to air pollution combined with GPS/GSM sensors. This range of new applications would be possible thanks to microsensors cheapness allowing simultaneously monitoring with a great number of microsensors, their low power consumption, absence of needed field maintenance/calibration.

However, due to reliability problems, there is a hesitancy to apply these microsensors for monitoring air pollution for legislative purposes. Microsensors have to be efficient, accurate, sensitive and reliable in addition to being small and inexpensive. Opportunely, in the last years, some technological progress took place and a few commercial microsensors are now available in the market. In fact, microsensors represent a promising indicative method for monitoring O_3 in ambient air to complement Ultra-Violet (UV) photometry[6], the O_3 reference method of measurement. Compared to other indicative method like diffusive sampling, microsensors show shorter response time, produce real time values without the need of analysis after sampling and need little power supply.

According to our previous laboratory and field study of O_3 microsensors[7], it appeared that:

- although experiments in exposure chambers under controlled conditions using synthetic gaseous mixtures can help to understand the chemical reaction paths at the sensitive surface of microsensors, the influence of chemical and meteorological parameters on their response, laboratory results are generally not reproduced with subsequent field monitoring of O_3 likely because of the different air matrixes of laboratory and fields;
- on the opposite, after field calibration by comparison of microsensor responses and UV-photometry measurements during a pre-campaign of about two-week, it was then possible to monitor O_3 with microsensor independently from UV photometry for 10 days at the EMEP station in Ispra (I).

To expand the conclusions of the first study, we carried out experiments at the end of summer 2010 at two sampling sites. At the first site, a rural site in Ispra (I), the microsensors were calibrated against UV photometry during a few days. Subsequently, the calibrated microsensors were taken to another rural site where the performance of the calibration function of Ispra site was evaluated. The trend of the differences between O_3 measured by UV photometry and microsensors were examined to evidence possible drift of the microsensors.

---

1 T. Takada, Ozone detection by In2O3 thin film gas sensor. In: T. Seiyama, Editor, Chem. Sensor Technology vol. 2 (1989), pp. 59–70 Kodansha, Tokyo/Elsevier, Amsterdam

2 E. Traversa, Y. Sadaoka, M. C. Carotta and G. Martinelli, Environmental monitoring field tests using screen-printed thick-film sensors based on semiconducting oxide, Sensors and Actuators B, Vol. 65, 1-3, 2000, 181-185

3 A. Schütze, N. Pieper and J. Zachejab, Quantitative ozone measurement using a phthalocyanine thin-film sensor and dynamic signal evaluation, Sensors and Actuators B: Chemical, Vol. 23, 2-3, 1995, 215-217.

4 M. Bobbia, V. Delmas, 'Honfleur, utilisation de micro-capteurs pour mesurer l'ozone, 22 mai au 27 aout 2003", Air Normand, Observatoire de la qualité de l'air/ALPA-REMAPPA, Rapport d'étude nº E01-01, http://www.airnormand.asso.fr

5 C. Pijolat, B. Riviere, M. Kamionka, J. P. Viricelle, P. Breuil, Tin dioxide gas sensor as a tool for atmospheric pollution monitoring: Problems and possibilities for improvements, JOURNAL OF MATERIALS SCIENCE 38 (2003) 4333 – 4346.

6 European Standard, 2005. EN 14625, Ambient Air Quality e Standard Method for the Measurement of the Concentration of Ozone by Ultraviolet Photometry. Brussels, Belgium.

7 M. Gerboles and D. Buzica, Evaluation of Micro-Sensors to monitor Ozone in Ambient Air, EUR 23676 EN, ISBN 978-92-79-11104-4, ISSN 1018-5593, DOI 10.2788/5978, 2009. ftp://pegasos:pegasos@ipscftp.jrc.it/erlap/ERLAPDownload.htm

The correlation of these differences with meteorological data were investigated to evidence possible interference and to propose new method of data treatment able to minimize the differences.

The measuring campaign at the second rural site was organized to evaluate O_3 damage to agriculture. Grape vine (*Vitis vinifera,* L.*)* is recognized as an ozone-sensitive crop. When the O_3 concentration in the atmosphere is high due to air pollution, important quantities of O_3 penetrate the vine leaf tissues through the stomata causing cell damage and interfering with the mechanisms of photosynthesis, with subsequent slowing down of the latter as a main consequence. The campaign was intended to test the performance of the fumigation facility and four open top chambers (OTC) were installed at a vineyard in Angera (northern Italy**)**.

2 Measuring campaigns

First, the microsensors sensors were installed for 3 days at the ABC-IS/EMEP station of the JRC Ispra for calibration (see Table 1). This monitoring station has been operating since 1985. Measurements performed at this station include meteorological parameters, gas phase species (SO_2, NOx, O_3 and CO) and particulate matter speciation. At the ABC-IS station, a UV Photometric Ambient Analyzer, model Thermo 49C is used to monitor O_3. It measures the absorption of O_3 molecules at a wavelength of 254 nm (UV light) in the absorption cell, followed by the use of Bert-Lambert law. At the station, calibration of O_3 analyzer is performed once a month using zero air taken from a gas cylinder and a span gas in the range 50 - 100 nmol/mol generated by a Thermo Envionment TEI 49C-PS transportable primary standard ozone generator yearly calibrated/check by the European Reference Laboratory of Air Pollution (ERLAP - JRC) and by TESCOM (Thermo Environment supplier in Italy). A Nafion Dryer system is connected to the O_3 instruments.

The measuring campaign took place in Angera, right after calibration, at a vine grape stand located in Angera (northern Italy, at 3 kilometer far from Ispra). Four OTCs were operated on the site, each one enclosing four vine plants (see Figure 1). Two OTCs were fed with ambient air containing comparable O_3 level as ambient air (called Not Filtered OTCs), whereas the two others were fed with filtered air, from which most of the ambient O_3 was removed (called Filtered OTCs) by a chemical substance (PURAFIL®). O_3 concentrations were monitored inside and outside the OTCs (both filtered and non-filtered) during the whole experiment, showing that the concentration in the filtered OTCs was about half the concentration inside the non-filtered ones. The instruments used to monitor O_3 concentration were the microsensors being validated in this study, NanoEnvi® ozone microsensors developed by Ingenieros Asesores S.A. (Llanera, Spain), and an O_3 UV photometry analyzer (Environmental Instruments, Inc. mod. TEI 49C).

Table 1: Sampling sites

Sampling sites	Available parameters	Date	Averaging time
Ispra (VA) Italy , ABC-IS/EMEP station	Air pollution and meteo	3-6 Sep. 2010	10 min
Angera (VA) Italy, rural site	O_3 and meteo	9 Sep.-1Oct. 2010	1 hour

Figure 1: Two open top chambers enclosing vine grape plants on the vineyard in Angera.

In Angera, O_3 measurements were carried out using a mobile laboratory placed alongside to the OTCs. It was equipped with the O_3 analyzer TEI 49C and an automatic switching valve connecting three 15–meter PTFE sampling tube. One line sampled ambient air, one line was connected to O_3-filtered OTC and the last one to a non-filtered OTC. The automatic valve switched of sampling line every 5 minutes allowing for 2 minutes of sampling line cleaning and O_3 measurements were averaged over the following 3 minutes. For each sampling line, O_3 concentrations was measured for 3 minutes every 15 minutes and subsequently converted to hourly averages.

Before the field measurements took place in Angera, the whole O_3 monitoring system consisting of the valves, 3 sampling tubes and the O_3 analyzer was calibrated in laboratory using the reference standard of ERLAP consisting in a Thermo Environment analyzer model 49 CPS cross checked with a NIST primary long path UV photometer. The O_3 monitoring system was calibrated in the range 0 – 150 nmol/mol (0, 50, 100 and 150 nmol/mol). The linear calibration function showed 3 slopes of 0.98 ± 0.01 and intercepts of -0.6 ± 0.6 nmol/mol.

Figure 2: NanoEnvi® ozone microsensors used to monitor ozone in grape vine OTC with their solar cells used for power supply

3 NanoEnvi Mote O_3, ozone continuous analyser based on nanotechnology

NanoEnvi O_3 Mote consists of several NanoEnvi Motes where each mote sends data to a coordinator unit using a suite of high level communication protocols based on low-power digital radios called ZigBee, like the standard IEE 802. 15.4. The coordinator unit can store data coming from different Motes, at same time, with a maximum of 128 motes per Coordinator. This main unit can manage different kinds of communication outputs like USB, RS232, or remote ones as Bluetooth, GSM/GPRS or FTP.

In the Network, the coordinator forms the root of the network tree and might bridge to other networks. There is exactly one ZigBee coordinator in each network since it is the device that initially launches the network. It is able to store information about the network, including acting as the Trust Centre and repository for security keys. By other hand, the Mote is an End Device with just enough functionality to tall to the parent node; it cannot relay data from other devices. This relationship allows the node to be asleep a significant amount of the time thereby giving long battery life.

Each NanoEnvi O_3 Mote is a small size, low power consumption, minimum maintenance and very low cost system for monitoring of O_3 at ambient levels. NanoEnvi O_3 Mote can be installed nearly everywhere since they can be powered by a little solar cell of only 5 Watt combined with a small 3.7 V Li-Ion battery. Most of the typical parameters in the mote are configurable, for example, the periodicity of data averages, with a minimum value of 1 minute or the triggering of electrical events when any limit values are breached.

In the present project, Ingenieros Asesores supplied a whole system consisting of:

- three NanoEnvi O_3 motes with solar panels for power supply (see Fig 2),
- one Coordinator datalogger for data storing and individual mote configuration,

- one ConfigNET PC software manufactured by Ingenieros Asesores for coordinator control, remote Motes configuration, data acquisition and storage of each mote.

As default, the motes provided by Ingenieros Asesores come with their own calibration coefficients for estimating ozone concentrations, including a temperature and humidity compensation, and a linear, second or third degree calibration factors.

The cost of each individual NanoEnvi Mote, with remote ZigBee communications and with battery and solar cell is the approx. 860 €, and the cost of the coordinator up to 128 motes, is the aprox. 1880 €. The cost of the hole network system with three points of ozone measurement is the aprox. 4460 €.

4 Sensors calibrations

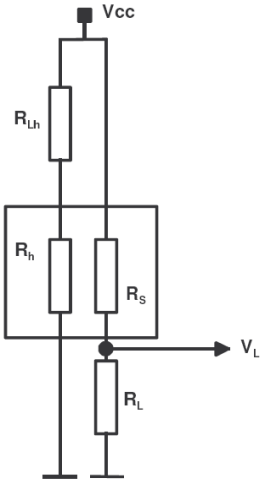

Figure 3: Sensor diagram

The microsensor probe consists in a micro-machined silicon structure equipped with a sensitive resistance (Rs) placed on top of a heating resistance (Rh) made of polysilicium. The microsensor probe is equipped with a load resistance playing the role of voltage divider. R_{LH} (see Figure 3) is used to limit the power consumption of the microsensor and to regulate the temperature of the sensitive layer (the target temperature for O_3 detection is about 400°C).The sensitive element is a thin layer of tin dioxide (SnO_2) which is deposited on top of the heater structure by dip-coating. These microsensors are already implemented by laboratories carrying out routine air pollution monitoring[8]. The manufacturer suggests the following equations to convert the sensor output signal into O_3 concentration:

$$R_S(1) = R\,e^{K(T-25)} \qquad (1)$$

$$O_3 = x_0 + x_1 R_S(2) + x_2 R_S^2(2) + x_3 R_S^3(2) \quad (2)$$

Where x_3, x_2, x_1 and x_0 are parameters specific to each microsensor given by the manufacturer. R, the resistance of the semiconductor in kOhms, is normalized to 25ºC using equation 1 where T is the ambient air temperature in ºC and K is the coefficient of the temperature correction (generally 0.05). The impedance characteristics of the SnO_2 semi-conductor are altered through reactions with the oxidizing gases present in the air. The detection mechanism can be modeled the following way:

$$\mathbf{O_3 + e^- \rightarrow O^- + O_2} \qquad (3)$$

In this sensitive layer oxidizing reaction, e^- is a conduction electron in the SnO_2 layer and O^- is a surface oxygen ion. The result of this oxidation is a reduction of the electron flow and thus an increase in the electric resistance of Rs. This reaction is totally reversible. The O_3 concentration is computed as the measured resistance Rs adjusted with the calibration and the temperature compensation parameters.

Experiments carried out in lab-exposure chamber[7] at constant temperature and steady O_3 concentrations showed that SnO_2 microsensors are sensitive to relative humidity (see Figure 4). Therefore, it is expected that equation 1 and equation 2 could need adjustment to reflect such interference.

Calibration should be carried out using the calibration function[9] (sensor resistance, Rs, versus O_3 concentrations levels) instead of the measurement function (O_3 concentrations levels versus sensor resistance, Rs) that is proposed by the manufacturer. We suggested using equation 4 according to the dependence of the residuals of the model on available parameters Pi (e.g. relative humidity or on the velocity of change of relative humidity) and the calibration function consisting in equation 5:

[8] A. Pérez-Junquera, A. Ayesta, M. Miñambres, L. García, and J. Blanco, "Ozone analyzer for Air quality monitoring based on semiconductor oxide sesnors", poster presented at the "Measuring Air Pollutants by Diffusive Sampling and Other Low Cost Monitoring Techniques, 15th -17Th September 2009, at the Krakow City House, Krakow, Poland

[9] ISO 6143:2001, Gas analysis - Comparison methods for determining and checking the composition of calibration gas mixtures, Geneva, Switzerland.

$$R_S(3) = R.e^{K(T-T_0)} - \left(\sum a_0.P_i + P_{i,m}\right) - \left(\sum a_1.\frac{dP_i}{dt} + a_2\right) - \qquad (4)$$

$$R_S(2) = x_0 + x_1 O_3 + x_2 O_3^2 + x_3 O_3^3 \qquad (5)$$

Where

- Rs is the resistance corrected for temperature and other parameters in kOhms,
- P_i is any influencing parameter (relative humidity, temperature, Rs(1), O_3 measured by UV photometry…),
- K is the coefficient of the temperature correction (initially set 0.05),
- T_0 is the average of ambient temperature in °C during the calibration period,
- $P_{i,m}$ is the average of influencing parameter P_i during the calibration period,
- a_0, a_1 and a_2 represent constants of the model that are fitted by weighted partial least square algorithms.

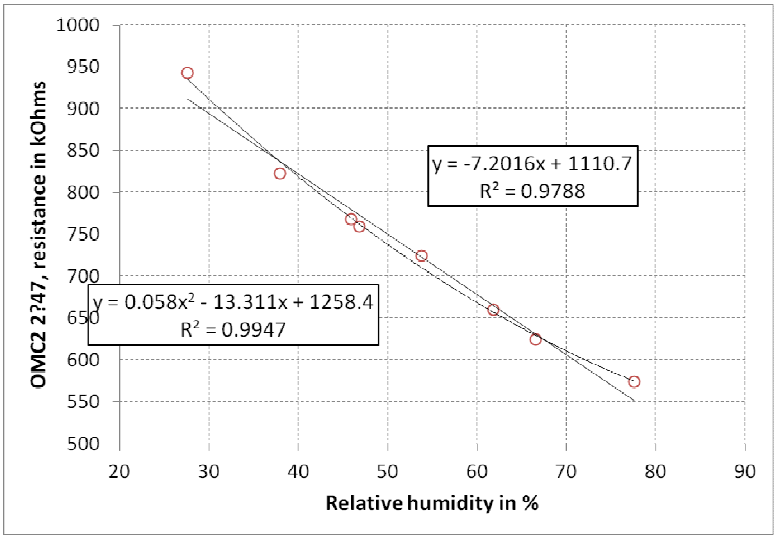

Figure 4: Laboratory experiments showing the decrease of resistance before normalization at 25 °C for an SnO_2 sensor. The ozone concentration and the temperaure of the air mixture were kept constant at 70 ± 0.4 nmol/mol and 25 ± 0.1 °C during experiments

In order to avoid the overwhelming importance of the abundant and scattered microsensor results at low O_3 during the fitting of the parameters, the average microsensor responses and their standard deviations were computed for successive lags of 5 nmol/mol. x_1 and x_0 were estimated by minimizing the weighted error function SSS (see equation 6). The calibration function of microsensors responses versus O_3 was generally linear, sometimes quadratic. The optimization algorithm used the following sum of square residuals equation assuming a linear model is :

$$SSS = \sum_{class=1}^{n} \frac{\sum_{class=1}^{n} n_i\, s_i^2(Rs_i)}{n_i\, s_i^2(Rs_i)} \left[\overline{Rs_i} - \left(x_0 + x_1.\overline{O_{3,i}}\right)\right]^2 \qquad (6)$$

Where

- n is the number of classes of 5 nmol/mol (0 to 5, 5 to 10, 10 to 15, …) with more than one valid measurements,
- $s_i(Rs_i)$ is the standard deviation of Rs values in the class i with n_i measurements,
- $\overline{Rs_i}$ *and* $\overline{O_{3,i}}$ are the averages of Rs and O_3 values in the class i.

5 Experimental Results

5.1 Calibration in Ispra

The three microsensors were warmed up for 48 hours before calibration took place. First, K was set to 0.05. Second, a first set of x_0, x_1, x_2 and x_3 parameters were estimated by minimization of equation 6. The order of the polynomial used for calibration was determined by observing the increase of the coefficient of determination of the polynomials giving Rs versus ozone measured by UV photometry. Then K was adjusted by maximizing the coefficient of correlation between O_3 calculated using equation 5 and O_3 measured by UV photometry. These two last steps (fitting of K and x_0, x_1, x_2 and x_3) were repeated until all these values converged through the iterations. K value was constrained between 0.02 and 0.1 and the slope and intercept of O_3 measured by UV photometry and microsensors were set to 1.00 ± 0.03 and 0 ± 3, respectively. At this point a last simultaneous optimization of K, x_0, x_1, x_2 and x_3 took place by minimizing the residuals between O_3 measured by UV photometry and the values obtained by solving equation 5.

Then the differences between Rs calculated with equation 1 and 5 were plotted against relative humidity, temperature, Rs calculated with equation 1, ozone measured by UV photometry and their first derivative over time. If a significant correlation between the residual of Rs and one parameter was detected, the constant values of equation 4 (a_0, a_1 and a_2) were fitted in order to minimize the ozone residuals starting with the parameters giving the highest effect.

5.1.1 NanoEnvi® 1

With the initial K value of 0.05 and after minimization of equation 6, a simple linear model ($Rs(2)_{kOhms}$ = -921 + 72.8.$O_{3,nmol/mol}$) could explain most of the variability of Rs(1) giving a Coefficient of Determination of 0.993 that did not significantly increase with a quadratic model (R^2 = 0,995, see Figure 5). Subsequently, the parameters x_0, x_1 and K were slightly modified to enhance the correlation between Rs(1) and O_3 measured by UV photometry and subsequently to diminish the differences of O_3 measured by UV photometry and with the microsensor (K = 0.06974, x_0 = -1118 and x_1.= 82,5). The standard error of the regression line of O_3 determined using equation 5 versus the one measured by UV photometry was $S_{y/x}$ = 3.1 nmol/mol. The relationship between the residuals Rs(1) - Rs(2) and the following parameters and their 1st derivative: relative humidity, temperature, Rs(1) and O_3 measured UV photometry are given in Figure 5.

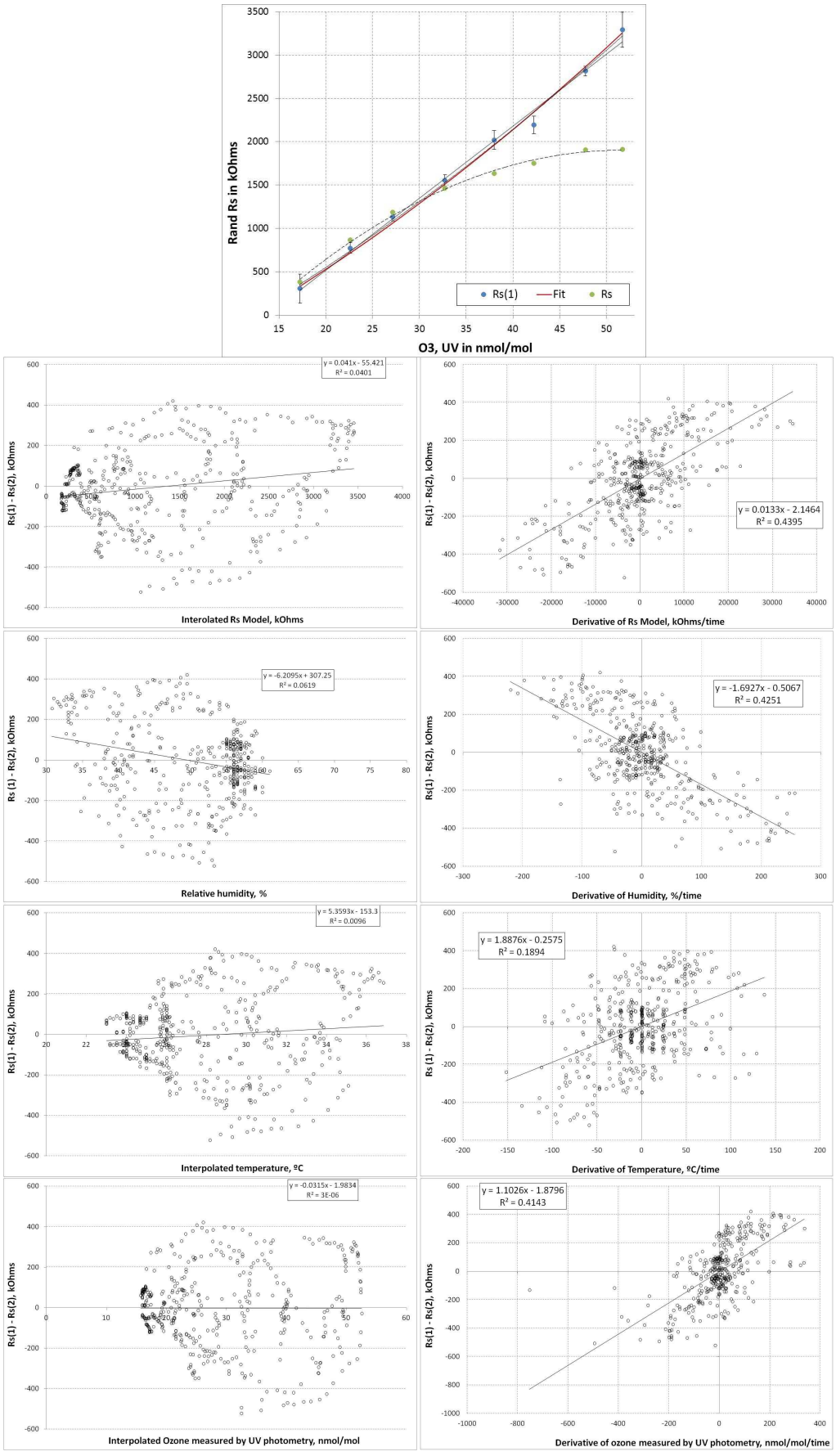

Figure 5: NanoEnvi 1, calibration of microsensor with K = 0.06974, x0 = -1118 and x1.= 82.5 (upper) where the y-axis error bars represent the 10-times magnified weights of equation 6. Scatter plot of the differences between Rs(1) and Rs(2) with some parameters and their first derivative over time: relative humidity, temperature, Rs(1) and ozone.

The differences between Rs(1) and Rs(2) values were slightly associated with the four parameters while they were more significantly associated with their derivative. As one could expected, the same behavior was observed for the derivative of Rs(1) and ozone that are two parameters highly correlated. The negative correlation with humidity may have come from the negative correlation between ozone and relative humidity. As these three parameters were correlated, it was decided to take dRs(1)/dt, the parameter showing the highest coefficient of determination. A final minimization of the standard error of the regression line of ozone measured by the microsensor and by UV photometry was $S_{y/x}$ = 2.6 nmol/mol model (from 2.6 to 2.0 nmol/mol, R^2 = 0.97) gave the following final equation for the determination of ozone:

$$R_S(3) = R.e^{K\,0.06974(T-27.9)} - \left(0.0138.{}^{dRs(1)}\!\!\diagup_{dt} - 2.1\right) - \qquad (7)$$

Leading to

$$O_3 = \frac{R.e^{0.06974(T-27.9)} - 0.0138\,{}^{dRs(1)}\!\!\diagup_{dt} + 1176}{82.5} \qquad (8)$$

Using equation 8, no significant correlation was found (see Figure 6) between Rs(3) – Rs(2) and the same parameters as in Figure 5. At the same time, the autocorrelation that could be observed for the four parameters in Figure 5 disappeared or was reduced as shows Figure 6

.

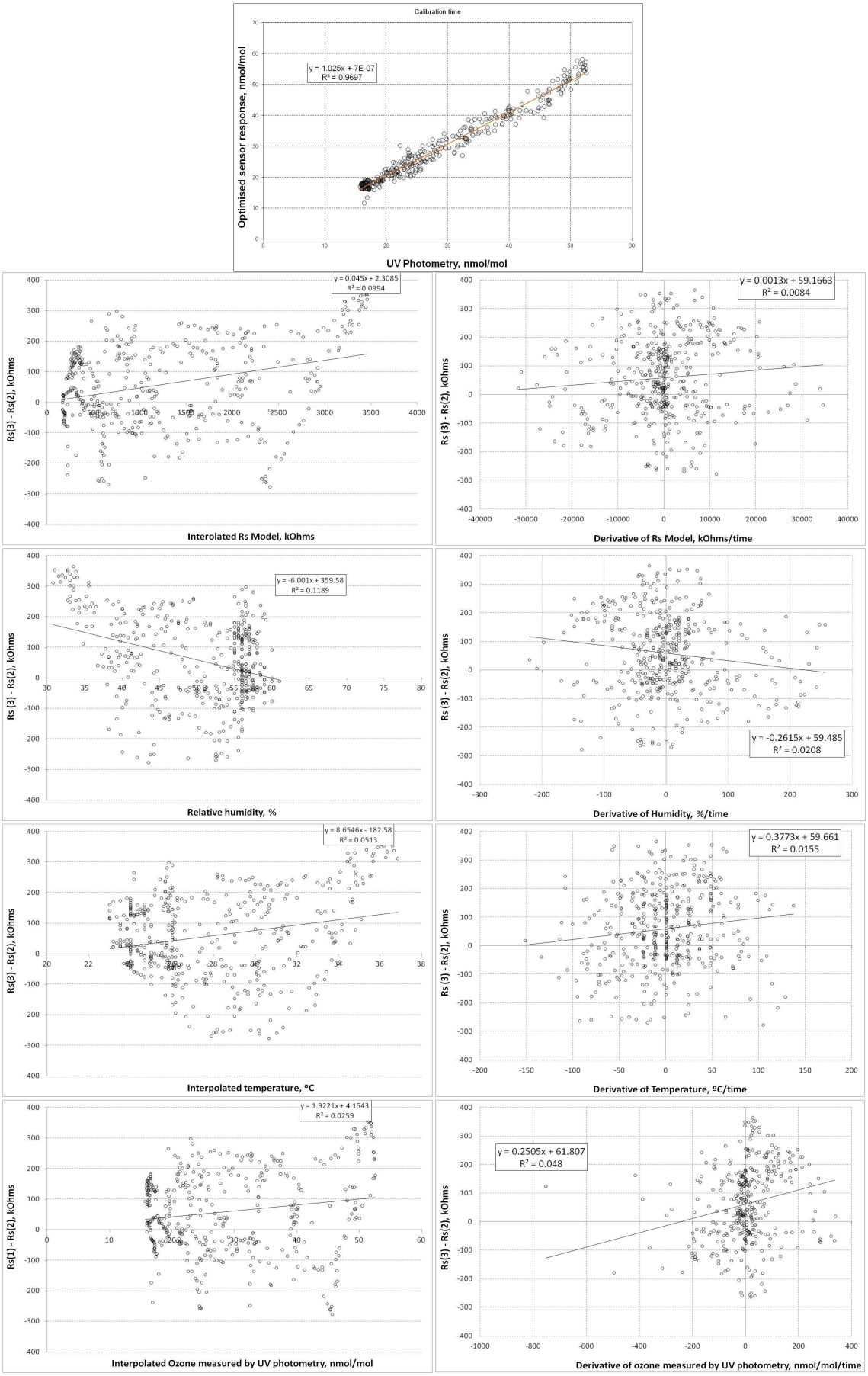

Figure 6: NanoEni®_1 Final calibration function (see equation 7, upper). Scatterplots of the differences between Rs(3) and Rs(2) and relative humidity, temperature, Rs(1) and ozone their first derivative over time showing the absence of correlation

5.1.2 NanoEnvi® 2

With the first K value of 0.05, we found a second order polynomial for Rs(2) (Rs(2) = -113 + 5.1 O_3 - 0.3073 O_3^2) with a mean of residuals between O_3 measured by UV photometry and with NanoEnvi® 2 of 2.7 nmol/mol and a coefficient of determination of R^2=0.9576. Subsequently, the parameters x_0, x_1, x_2 and K were slightly modified to increase the correlation between O_3 measured by UV photometry and with NanoEnvi® 2 leading to K = 0.09317, x_0 = 170, x_1.= -20.9 and x_2.= -0.8307 (with R^2= 0.9638). The standard error of the regression line of O_3 determined using equation 5 and measured by UV photometry was $S_{y/x}$ = 2.5 nmol/mol. Figure 7 shows a significant improvement of the agreement between Rs(1) and O_3 measured by UV with a quadratic model instead of a linear model.

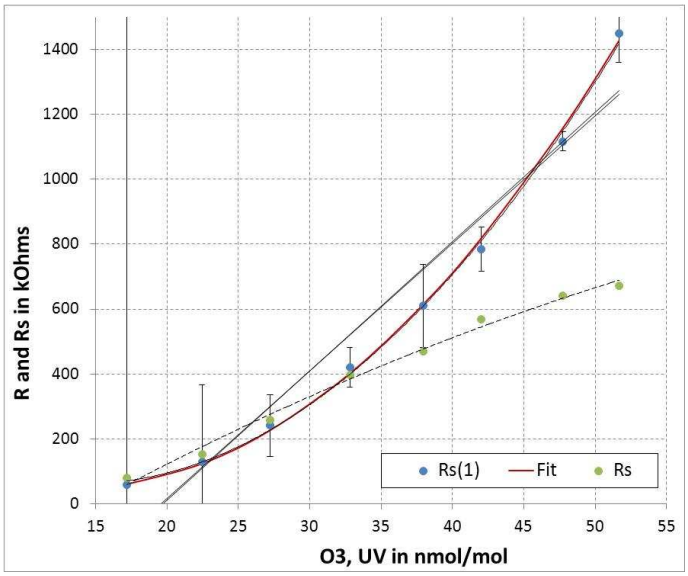

Figure 7: NanoEnvi®_2, relationship of resistance versus ozone measured by UV photometry. The error bars represents the 10-time magnified weights calculated according to equation 6.

The relationship between the residuals Rs(1)-Rs(2) from the one hand and relative humidity, temperature, Rs(1) and O_3 measured by UV photometry and their derivatives from the other hand, showed again significant correlations mainly with the derivative of the four parameters with R^2 of 0.15, 0.03, 0.13 and 0.11 for the derivatives of Rs, temperature, relative humidity and O_3, respectively. Using dRs(1)/dt for the correction of Rs(1) gave the following final equation for the determination of ozone:

$$R_S(3) = R.e^{K\,0.09317(T-28.6)} - \left(0.00864\,{dRs(1)}/{dt} + 2\right) - \qquad (9)$$

Leading to

$$O_3 = \frac{20.9 + \sqrt{20.9^2 - 3.322(168 - Rs(3))}}{1.661} \qquad (10)$$

The calibration function obtained using equation 10 is given in Figure 8. Using equation 9, no significant correlation was found between Rs (3) – Rs (2) and the four parameters and their 1st derivative. At the same time, the autocorrelation function that could be observed before for the four parameters disappeared or was reduced.

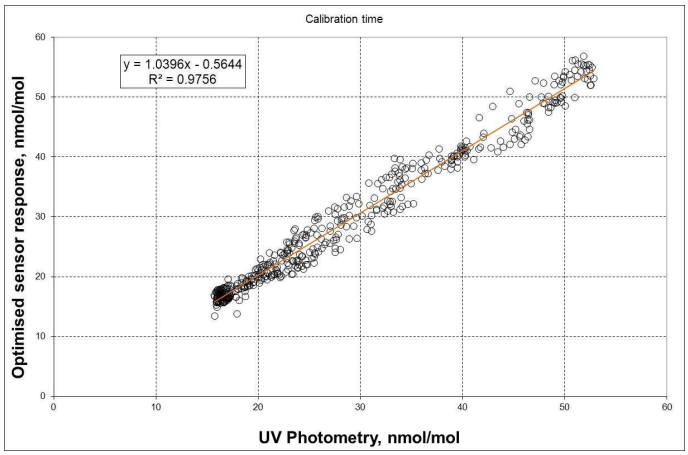

Figure 8: NanoEnvi 2. Final calibration function. Ozone was estimated with Rs (3)

5.1.3 NanoEnvi® 3

The initial K value of 0.05 leads to a simple linear model Rs(2) = -839 + 59.4 O_3 which was sufficient to account for most of the variability of Rs(1) (see Figure 9) with a mean of residuals between UV and NanoEnvi® 3 of 3.3 nmol/mol (R^2= 0.93). Afterwards, the parameters x_0, x_1 and K were slightly modified to increase the correlation between O_3 measured by UV photometry and with the microsensor (K = 0.07352, x_0 = -1079 and x_1.= 69.7). The standard error of the regression line of ozone determined using equation 5 and measured by UV photometry was $S_{y/x}$ = 3.1 nmol/mol (R^2 = 0.94).

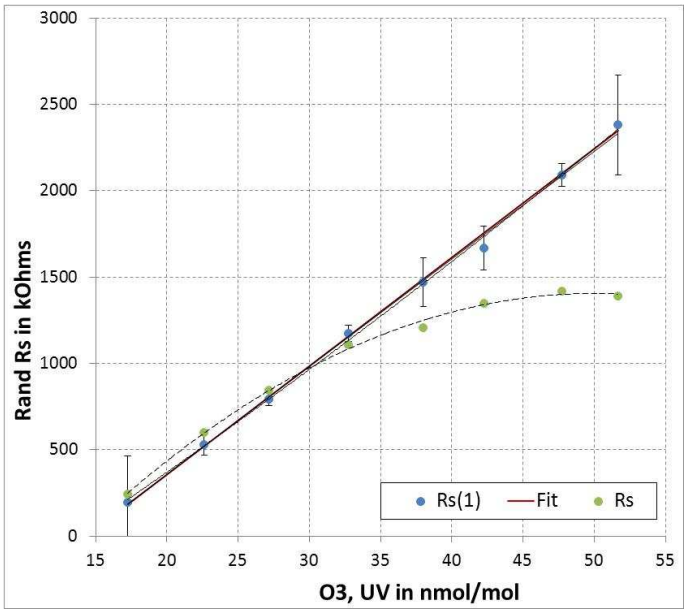

Figure 9: Calibration of NanoEnvi® 3 microsensor: initial fitting of x0 and x1 with K set to 0.05 (upper left) where the y-axis error bars represent the 10-times magnified weights of equation 6

Like for the NanoEnvi® 1 and 2, the relationship between the residuals Rs(1)-Rs(2) from the one hand and relative humidity, temperature, Rs(1) and O_3 measured UV photometry and their derivatives from the other hand, were once again not associated with any of these parameters but with their derivatives with R^2 of 0.36, 0.38, 0.18 and 0.35 for the derivatives of Rs, temperature, relative humidity and O_3, respectively. Taking dRs(1)/dt into account, gave the following final equation for the determination of ozone:

$$R_S(3) = R.e^{K\,0.07352(T-28.2)} - \left(0.00143\,{}^{dRs(1)}\!/_{dt} - 2.0\right) \qquad (11)$$

Leading to

$$O_3 = \frac{R.e^{0.07351(T-28.2)} - 0.0143^{dRs(1)/dt} + 1087}{70} \qquad (12)$$

The calibration function obtained using equation 12 is given in Figure 10. Using equation 11, the standard error of the regression line of ozone was reduced to $S_{y/x}$ = 2.5 nmol/mol (R^2=0.962) and no significant correlation was found between Rs(3) – Rs(2) and the following parameters and their 1st derivative: relative humidity, temperature, Rs(1) and O_3 measured UV photometry. At the same time, the autocorrelation that could be previously observed for the four parameters disappeared or was reduced.

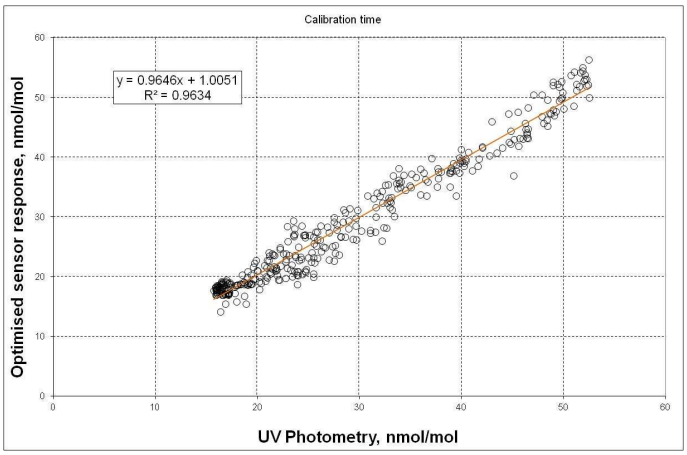

Figure 10: NanoEnvi® 3. Final calibration function. Ozone was estimated with Rs(3)

5.2 Measuring campaign in Angera

5.2.1 Application of the Ispra's calibrations

The NanoEnvi 2 and 3 were connected to the two O_3-filtered OTCs while the NanoEnvi® 1 was connected to a non filtered OTC. In Angera, the microsensors were warmed up for 48 hours before starting the data acquisition. Among the two O_3-filtered OTCs, O_3 monitoring with UV photometry took place only in the OTC where NanoEnvi 2 was placed and the same data were also used for the data treatment of the measurements of NanoEnvi 3. NanoEnvi 2 had a failure in the data acquisition and transfer from September 20th until the end of the measuring campaign.

For each microsensor, O_3 in Angera was estimated using the calibration functions established during the Ispra calibration experiments. Figure 11, Figure 12 and Figure 13 for NanoEnvi 1,2 and 3, respectively, show the trend of daily and hourly residuals between ozone measured by UV photometry and microsensors (using Rs(3)) in Ispra and Angera. The main observation is the appearance of a positive bias for the microsensors measurements in Angera for the three sensors:

- For NanoEnvi 1, the differences between microsensor and UV photometry values changed from -0.5 ± 2.4 nmol/mol in Ispra to 10.7 ± 2.7 nmol/mol in Angera for daily residuals and from 0.2 ± 2.7 to 10.8 ± 4.8 nmol/mol for hourly residuals.
- For NanoEnvi 2, the differences changed from -0.5 ± 1.3 nmol/mol to 19.0 ± 2.8 nmol/mol for daily residuals and from 0.2 ± 2.7 to 19.1 ± 4.5 nmol/mol for hourly residuals.
- For NanoEnvi 3, the differences changed from -1.7 ± 3.3 nmol/mol to 18.5 ± 3.1 nmol/mol for daily residuals and from -0.6 ± 3.4 nmol/mol to 18.8 ± 5.2 nmol/mol for hourly residuals. The differences in Angera were calculated until Sep. 24th because the residuals of NanoEnvi 3 had an important decrease starting on that day. Between 24-26 Sep, a rapid change of temperature, relative humidity and O_3 took place (see Figure 13) and the microsensor stopped working. After a data transfer on Sep 26, the microsensor started working again although its responses became considerably lower than the one of UV photometry (see Figure 13). This can also be observed in the 2nd scatter plots of Figure 13 where the microsensor measurements after 26 Sep appear under the regression line.

Nearly the same magnitude of daily and hourly biases was observed though with a higher scattering for the hourly data. The physical origin of this bias is not very clear.

Applying the correction of the derivative of Rs(1) determined in Ispra to the data of Angera did not improve the agreement between O_3 measured by UV photometry and microsensors. If one consider the sensor data between 15 and 24 September, the coefficient of determination of NanoEnvi 3 is rather high ($R^2 = 0.87$) even though the reference measurements by UV photometer were sampled into OTC n. 2.

The coefficient of determination is lower for NanoEnvi 2 than for the other sensors. However the time series of NanoEnvi 2 being shorter, it cannot be compared with the one of NanoEnvi 1 or 3. Comparing NanoEnvi 1 from the one hand and NanoEnvi 2/3 from the other hand, the extent of the bias in Angera is also different for the two groups of microsensors (10 nmol/mol against 18 nmol/mol, respectively). This difference could be explained by the different air matrix in the OTCs since NanoEnvi 2 and 3 were placed in the O_3-filtered OTCs while NanoEnvi 1 was placed in the non filtered OTC.

Trying to explain the bias between Ispra and Angera, we first observed the daily time series of O_3 and meteorological parameters in both sampling sites. Looking at Figure 11, one may observe that relative humidity had similar daily minimum and maximum values at the two sites with slight higher daily averages in Angera. On the opposite, O_3 and temperature were lower in Angera compared to Ispra with a slight decreasing trend. However, looking at the correlation between the residuals of O_3 estimated by microsensors with temperature, relative humidity and O_3 measured by UV photometry did not give any clear indications: for the NanoEnvi 1 the residuals were strongly correlated with O_3 measured by UV photometry ($R^2 = 0.70$), for NanoEnvi 2 they were correlated with relative humidity ($R^2 = 0.50$) while the residuals of NanoEnvi 3 showed a weak correlation with temperature. NanoEnvi 2 measurements showed a clear daily drift of about -1.1 nmol/mol. With such variable observations, it was not possible to draw conclusions.

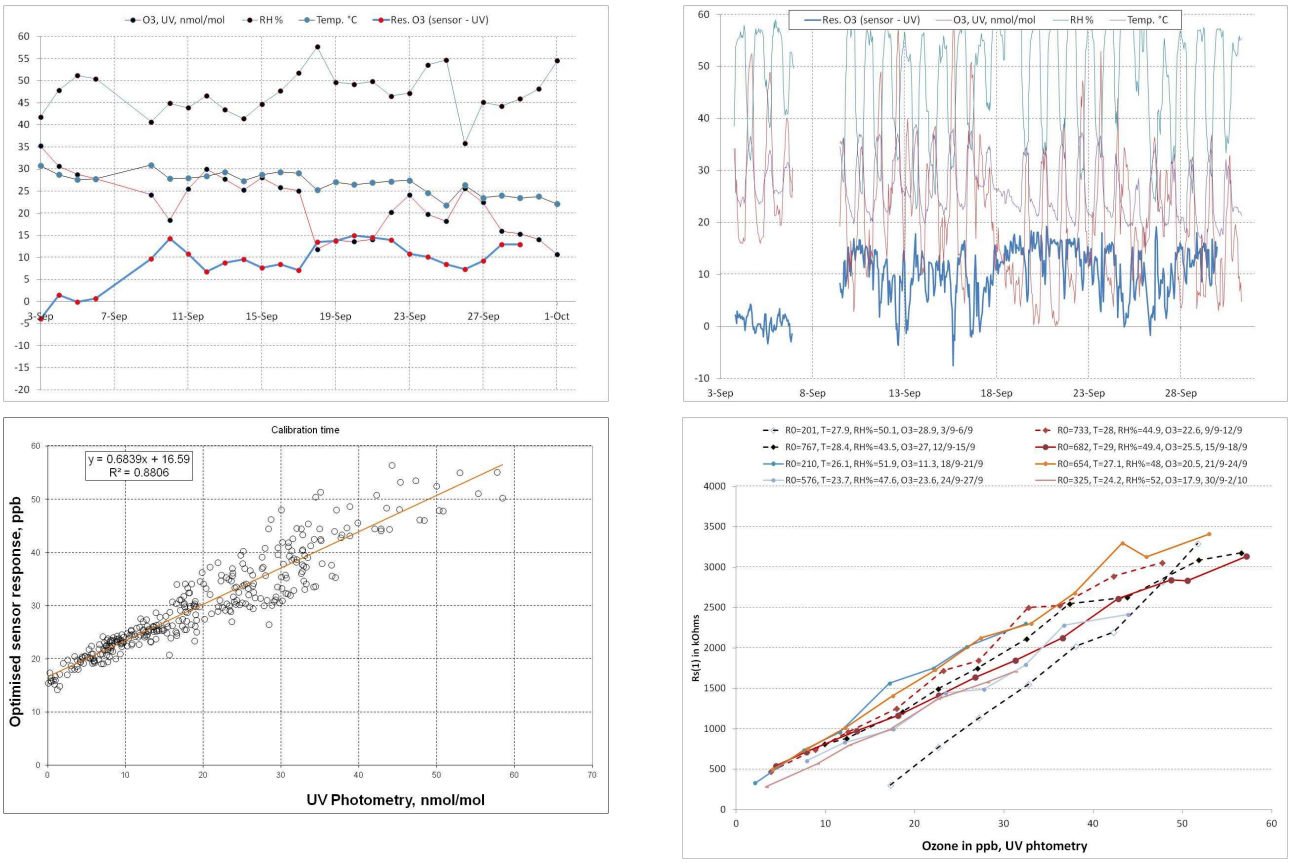

Figure 11: NanoEnvi 1; Upper left; trend of O_3, temperature and relative humidity and daily differences between O_3 measured by UV photometry and microsensor (Rs(3)) in Ispra and Angera. Upper right: same trend for hourly measurements. Lower left: scatter plot of O_3 estimated by microsensors versus O_3 measured by UV photometry. Lower right: Rs(1) versus ozone concentration measured by UV photometry every 3 days. The 1st line corresponds to the calibration experiments in Ispra while the other ones are the microsensor responses in Angera.

Looking at the scatter plots of O_3 estimated by NanoEnvi 1, 2 and 3 in Angera versus O_3 measured by UV photometry, an increase of the scattering for O_3 higher than 20 nmol/mol can be observed (see Figure 11, Figure 12 and Figure 13). This behavior could be explained by an inadequate temperature correction (K factor determined in Ispra using equations 7, 9 and 11) that produced noisy estimation at temperature corresponding to O_3 concentrations higher than 20 nmol/mol in Angera. No easy solution could be found to solve this problem even though trying to modify both coefficients K and T_0.

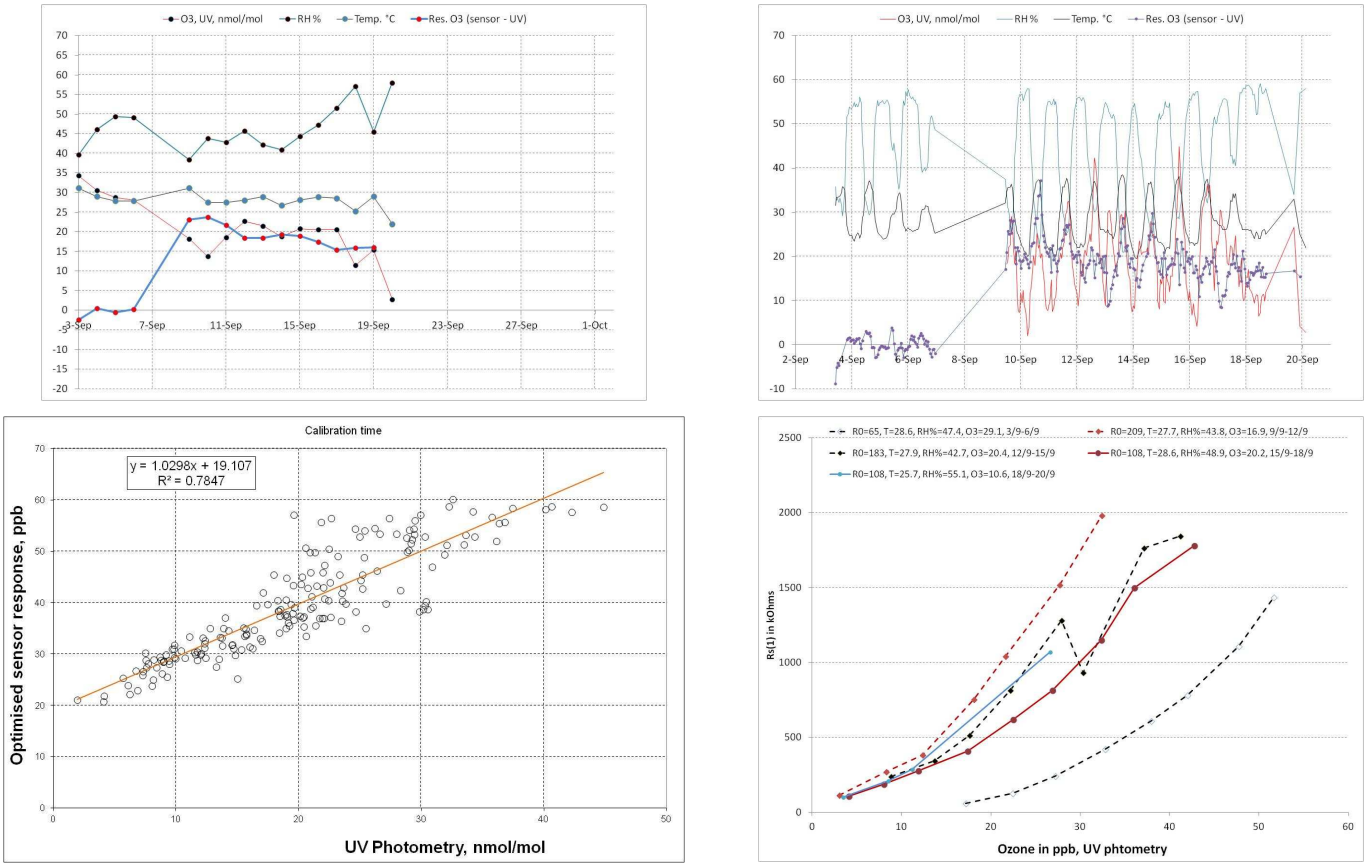

Figure 12: NanoEnvi 2; Upper left; trend of O_3, temperature and relative humidity and daily differences between O_3 measured by UV photometry and microsensor (Rs(3)) in Ispra and Angera. Upper right: same trend for hourly measurements. Lower left: scatter plot of O_3 estimated by microsensors versus O_3 measured by UV photometry. Lower right: Rs(1) versus ozone concentration measured by UV photometry every 3 days. The 1st line corresponds to the calibration experiments in Ispra while the other ones are the microsensor responses in Angera.

For NanoEnvi 1, the O_3 residuals in Angera (microsensor –UV) did not show a significant drift over time. The scatter plot of O_3 estimated by the microsensor versus the one measured by UV photometry (see Figure 11) shows an intercept of about 16.5 nmol/mol with a slope of about 70 %. Moreover, when looking at Rs(1) versus O_3 measured by UV photometry every three days (see Figure 11, Figure 12 and Figure 13), we can clearly observe different lines in Ispra and Angera, with equal sensor resistances corresponding to O_3 concentrations about 15 nmol/mol higher in Ispra than in Angera for the three microsensors. The lines of Rs versus O_3 measured by UV photometry show a different slope in Ispra and in Angera for NanoEni 1. This indicates that a simple correction of the coefficient x_0 of equation 5 (for example by determining the average minimum resistance at night time) would not be successful since the calibration lines in Ispra and Angera were not parallels.

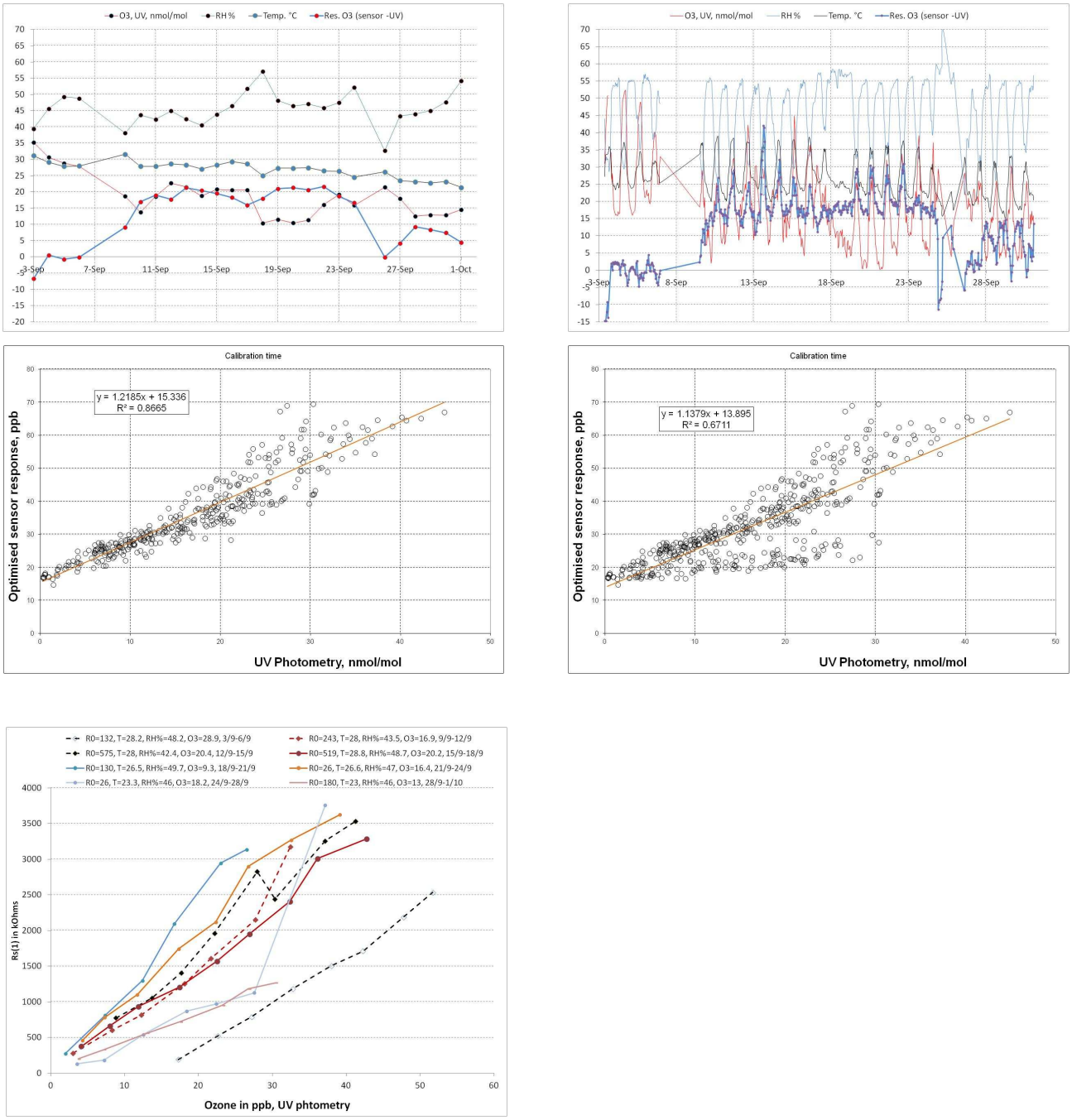

Figure 13: NanoEnvi 3; Upper left; trend of O_3, temperature and relative humidity and daily differences between O_3 measured by UV photometry and microsensor (Rs(3)) in Ispra and Angera. Upper right: same trend for hourly measurements. Middle: scatter plot of O_3 estimated by microsensors versus O_3 measured by UV photometry between 15-24 Sep (left) and between 15 Sep. – 1 Oct (right). Lower: Rs(1) versus ozone concentration measured by UV photometry every 3 days. The 1st line corresponds to the calibration experiments in Ispra while the other ones are the microsensor responses in Angera.

Calibrating the microsensors in Ispra and then measuring in Angera did not give a lot of success mainly because of the bias between Ispra and Angera sites presented here before. However, when calibrating the microsensor values using measurements of the 6 first days in Angera (9 to 15 Sep.), better agreements with UV photometry were obtained. Six days were necessary to get sufficient data for calibration in Angera where only hourly data were available. For NanoEnvi 1 microsensor, a quadratic relationship between Rs(1) and O_3 was observed leading to the equation:

$$O_3 = \frac{-60 + \sqrt{60^2 + 1.17(349 - R.e^{0.04682(T-28.4)})}}{-0.292} \qquad (13)$$

With this equation, the mean daily and hourly residuals between 16 Sep. and 1 Oct were -0.7 ± 2.3 nmol/mol and -0.5 ± 3.9 nmol/mol, respectively .

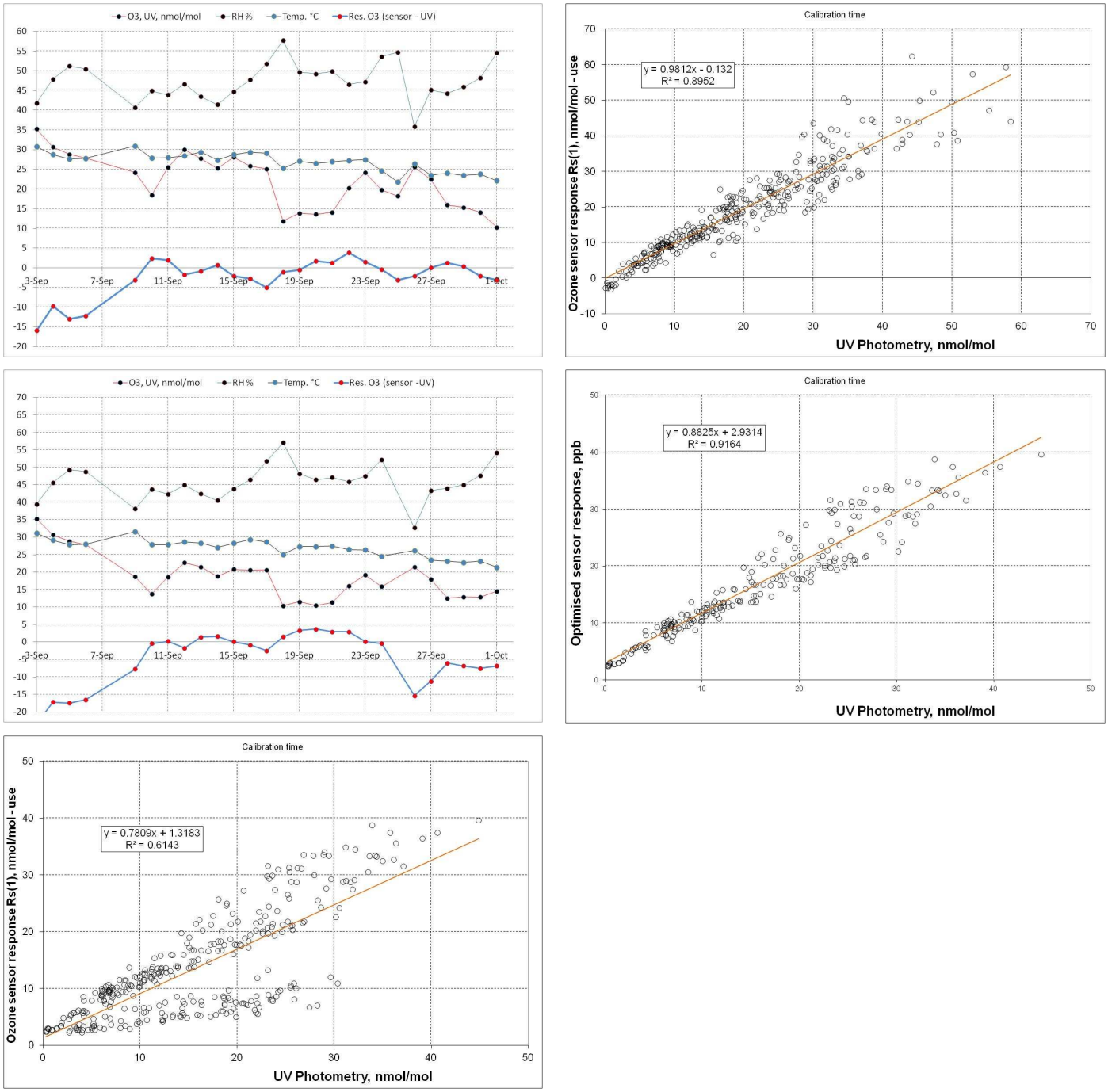

Figure 14: Upper: residuals and scatterplot of hourly averages between 16 Sep. and 1 Oct. for NanoEnvi 1 calibrated in Angera between 9 and 15 Sep.. Middle: residuals and scatterplot of hourly averages between 16 and 24 Sep. for NanoEnvi 3 calibrated in Angera between 9 and 15 Sep. Lower: scatterplot of hourly averages between 16 Sep. and 1st Oct. for NanoEnvi 3 calibrated in Angera between 9 and 15 Sep.

No data treatment was carried out for the NanoEnvi 2 because the time series ended on 18 Sep and was not enough long. For the NanoEnvi 3 microsensor, a linear relationship between Rs(1) and O_3 was observed leading to the equation

$$O_3 = \frac{R.e^{0.06550(T-27.7)} + 1158}{89.4} \qquad (14)$$

With this equation, the mean daily and hourly residuals between 16 Sept and 24 Sep were -0.3 ± 2.3 nmol/mol and -0.5 ± 3.6 nmol/mol , respectively. Between 26 Sep and 1 Oct, the decrease of microsensor response was again observed (see Figure 14, graphs n. 3, 4 and 5). Substantial changes of the parameters of equations 7, 8 and 11, 12 were needed to reach this result. Conversely to what was observed with the calibration in Ispra, the residuals between Rs(1) and Rs(2) were not highly correlated with any parameters or derivative of parameters.

5.2.2 Use of neural network

Neural networks are often successfully applied across an extraordinary range of problem domains. Neural networks are very sophisticated modeling techniques, capable of modeling extremely complex functions. In particular, neural networks are non-linear. Neural networks learn by example. The neural network user gathers representative data, and then invokes training algorithms to automatically learn the structure of the data. Neural networks are also intuitively appealing, based as they are on a crude low-level model of biological neural systems.

O_3 concentrations measured by UV photometry during the Ispra experiment were used as dependent variable, leading to 432 (24x3x6) cases to build the neural network (two thirds for training and one third for testing the network). The neural network was then validated using the measurements of the Angera experiment. Neural network provided an easy solution to include input variables like the date (proxy of the microsensor drift), the first derivatives of any parameter or relative humidity. RH is that is known to be important but it is difficult to include into a resistance deterministic model like the one of the manufacturer.

Table 2: Correlation matrix in Ispra, italic font indicates significant coefficient of correlations, Marked correlations are significant at p < .05000 N=382. The values of the first diagonal give the standard deviation of each parameter

	Means	O_3, UV nmol/mol	T, °C	RH,%	Rs kOhms	R/R_0	Daily R_0 kOhms	dHr/dt %/time	dRs/dt kOhms/time	dT/dt °C/time
O_3,	29.84	11.6	*0.94*	*-0.92*	*0.90*	*0.87*	0.03	*0.14*	-0.09	-0.02
T	28.48	*0.94*	3.8	-0.94	*0.83*	*0.85*	-0.03	0.10	0.00	0.02
RH	49.22	*-0.92*	*-0.94*	8.2	*-0.83*	*-0.84*	0.03	0.04	-0.08	*-0.16*
Rs	1110.13	*0.90*	*0.83*	*-0.83*	593.3	*0.84*	*0.22*	-0.00	0.05	0.03
R/R_0	4.07	*0.87*	*0.85*	*-0.84*	*0.84*	2.5	*-0.25*	0.04	-0.01	0.01
Daily R_0	290.29	0.03	-0.03	0.03	*0.22*	*-0.25*	111.4	-0.06	*0.21*	-0.02
dHr/dt	-2.32	*0.14*	0.10	0.04	-0.00	0.04	-0.06	81.5	*-0.70*	*-0.82*
dRs/dt	632.71	-0.09	0.00	-0.08	0.05	-0.01	*0.21*	*-0.70*	6140.2	*0.48*
dT/dt	1.27	-0.02	0.02	*-0.16*	0.03	0.01	-0.02	*-0.82*	*0.48*	38.9

The input data consisted of Rs, temperature, relative humidity, and the derivative of these 3 parameters, daily minimum resistance (daily R_0), Rs/R_0 ratio and date. Several architectures of neural network were evaluated: multiLayer Perceptron (MLP)[10], radial basis function (RBF)[11] and generalized regression neural network (GRNN)[12]. The first attempt included the following input variables: temperature, relative humidity, microsensor resistance and the derivative of these three parameters, minimum daily resistance (R_0), Rs/R_0 and excel transformed date. To limit the number of input variables and the over-learning of the data noise by the neural network while still using the necessary explicative variables, only the variables having the biggest standard deviation and smallest coefficient of correlation between each other were included in the network (see Table 2).

With all parameters included, the neural networks were not very successful to predict the data of the validation set, yielding a coefficient of correlation of about 0.88. Sensitivity analysis was used in order to assess the importance of each to the respective (fitted) models. Given a fitted model with certain model parameters for

[10] Bishop, C. (1995). Neural Networks for Pattern Recognition. Oxford: University Press.

[11] *Haykin, S. (1994). Neural Networks: A Comprehensive Foundation. New York: Macmillan Publishing.*

[12] *Speckt, D.F. (1991). A Generalized Regression Neural Network. IEEE Transactions on Neural Networks 2 (6), 568-576.*

each input variable, we determined what the effect of varying the parameters would be on the overall model fit. We computed the Sums of Squares residuals when the respective input variables were eliminated from the neural network. The predictors (in the results table) were then sorted by their importance or relevance for the particular neural net. The input variables were thus limited in order of importance to Rs, relative humidity, temperature, dT/dt and dRs/dt.

The best results were obtained using the MLP with 5 input variables (Rs, T, RH, dT/dx, dRs/dx) and 3 hidden nodes in one hidden layer. The Quasi-Newton training algorithm was used as the optimization algorithm. The coefficient of determination of O_3 estimated with the neural network and O_3 measured by UV photometry for the validation set of the network was 0.884 quite similar to the one obtained with the deterministic model (0.881, see Figure 11) and with very similar regression line, both for the slope and intercept of its equation. Therefore, using neural network, we confirmed the presence of a bias between the data of Ispra and Angera (see Figure 15).

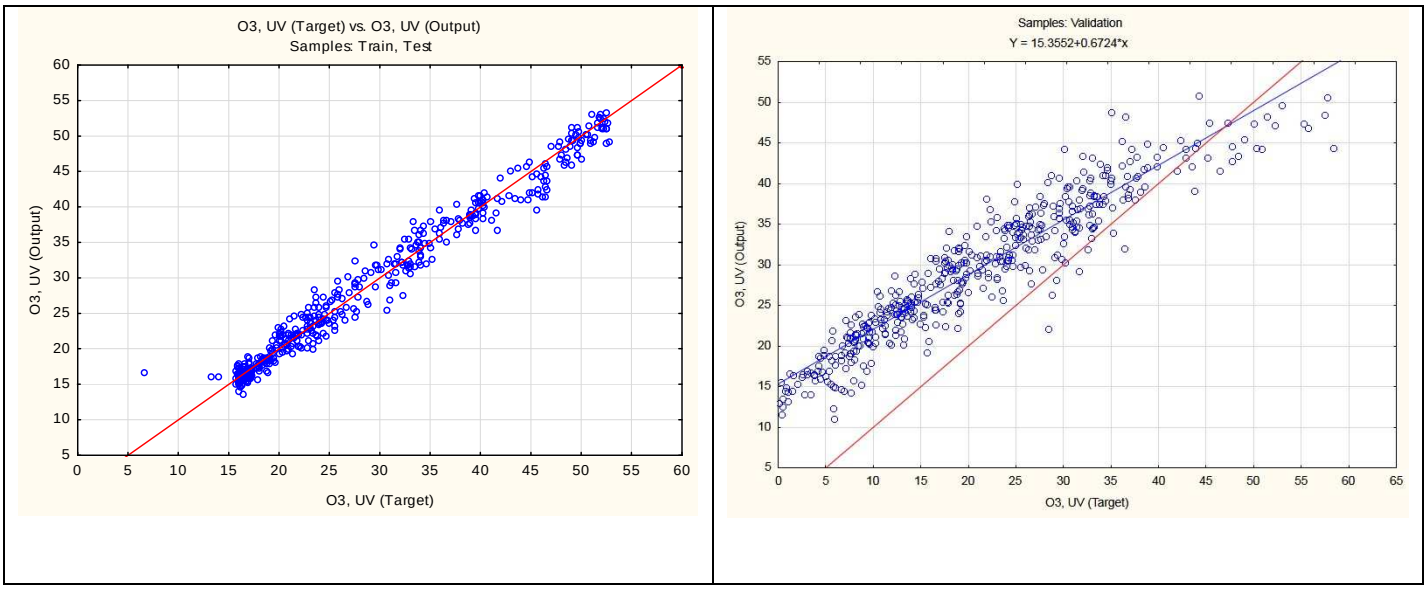

Figure 15: Ozone determined by the neural network (Multi Layer Perceptron 5 input variables, 3 hidden nodes) of the training set (in Ispra) and validation set (in Angera)

6 Discussion and conclusions

- Calibration functions determined in Ispra could not be directly applied to the microsensor measurements in Angera.
- The main finding of the campaign, which aimed verifying the possibility to calibrate the microsensors at one site followed with ozone monitoring at another site, is the detection of a bias between calibration in Ispra and measurements in Angera. At low ozone concentrations, this bias was about 15 nmol/mol. However, errors of the reference method of measurement either in Ispra or Angera cannot be excluded.
- The bias could not be simply eliminated by a re-zero calibration of microsensors because its magnitude depended on the ozone concentration.
- If the calibration was carried out with 6-day measurements in Angera, the microsensors were rather successful with daily bias in the range of 1 ± 2.3 nmol/mol and hourly bias in the range of 0.5 ± 4 nmol/mol.
- The magnitude of the bias and its relationship with ozone levels were different in the O_3-filtered OTC and in the un-filtered OTC suggesting a different matrix effect of ambient air on the microsensor response.
- For one microsensor, a sudden and abrupt change in the calibration function determined in Angera took place at the end of the measuring campaign and we could not determine the cause.

- Calibration should be carried out on the calibration function Rs = f(O_3) and not the analysis function O_3 =f (Rs). Generally, simple linear models are sufficient for the calibration function once Rs is corrected for temperature effect. In some occasion 2nd order models are necessary. In Ispra, the calibration function could be optimized by introducing a correction of the 1st derivative of Rs. However, it was found that this sophisticated approach did not produce any improvement for the experiments in Angera.

European Commission

EUR 25156 EN – Joint Research Centre – Institute for Environment and Sustainability

Title: Field evaluation of NanoEnvi microsensors for ozone monitoring

Author(s): M. Gerboles, I. Fumagalli, F. Lagler and S. Yatkin

Luxembourg: Publications Office of the European Union

2012 – 24 pp. – 21.0 x 29.7 cm

EUR - Scientific and Technical Research series - ISSN 1831-9424 (online), ISSN 1018-5593 (print)

ISBN 978-92-79-22682-3

doi:10.2788/44968

Abstract

Previous studies have showed that microsensors can successfully measure ozone in ambient air for a limited period of time after on-site calibration by comparison to ultraviolet photometry. This method is generally more successful than the calibration in exposure chambers under controlled conditions because of the difference between laboratory and fields air matrixes.

To expand this result, we carried out an experiment at two sampling sites. At the first site, the microsensors were calibrated during a few days. Subsequently, the calibrated microsensors were taken to another sampling site where the effectiveness of the calibration function of the first site was evaluated. The trend of the differences between UV photometry and microsensors were analyzed to evidence possible drift of the microsensors over time. The correlation of these differences with meteorological data was investigated to evidence possible interference and to propose new calibration methods.

The mission of the JRC is to provide customer-driven scientific and technical support for the conception, development, implementation and monitoring of EU policies. As a service of the European Commission, the JRC functions as a reference centre of science and technology for the Union. Close to the policy-making process, it serves the common interest of the Member States, while being independent of special interests, whether private or national.

LB-NA-25156-EN-N